

## Three-dimensional structure of echistatin and dynamics of the active site

Yuan Chen<sup>a</sup>, Asif K. Suri<sup>a</sup>, Dorothea Kominos<sup>a</sup>, Gautam Sanyal<sup>b</sup>, Adel M. Naylor<sup>b</sup>, Steven M. Pitzenberger<sup>b</sup>, Victor M. Garsky<sup>b</sup>, Ronald M. Levy<sup>a,\*</sup> and Jean Baum<sup>a,\*</sup>

<sup>a</sup>Chemistry Department, Rutgers University, Piscataway, NJ 08855, U.S.A.

<sup>b</sup>Departments of Medicinal Chemistry, Molecular Systems and Pharmaceutical Research, Merck Research Laboratories, West Point, PA 19486, U.S.A.

Received 6 August 1993

Accepted 19 October 1993

*Keywords:* Echistatin; Structure; Dynamics; Arg-Gly-Asp (RGD)

---

### SUMMARY

The snake venom protein echistatin contains the cell recognition sequence Arg-Gly-Asp and is a potent inhibitor of platelet aggregation. The three-dimensional structure of echistatin and the dynamics of the active RGD site are presented. A set of structures was determined using the Distance Geometry method and subsequently refined by Molecular Dynamics and energy minimization. Disulfide pairings are suggested, based on violations of experimental constraints. The structures satisfy 230 interresidue distance constraints, derived from nuclear Overhauser effect measurements, five hydrogen-bonding constraints, and 21 torsional constraints from vicinal spin-spin coupling constants. The segment from Gly<sup>5</sup> to Cys<sup>20</sup> and from Asp<sup>30</sup> to Asn<sup>42</sup> has a well-defined conformation and the Arg-Gly-Asp sequence, which adopts a turn-like structure, is located at the apex of a nine-residue loop connecting the two strands of a distorted  $\beta$ -sheet. The mobility of the Arg-Gly-Asp site has been quantitatively characterized by <sup>15</sup>N relaxation measurements. The overall correlation time of echistatin was determined from fluorescence measurements, and was used in a model-free analysis to determine internal motional parameters. The active site has order parameters of 0.3–0.5, i.e., among the smallest values ever observed at the active site of a protein. Correlation of the flexible region of the protein as characterized by relaxation experiments and the NMR solution structures was made by calculating generalized order parameters from the ensemble of three-dimensional structures. The motion of the RGD site detected experimentally is more extensive than a simple RGD loop ‘wagging’ motional model, suggested by an examination of superposed solution structures.

---

### INTRODUCTION

Platelets adhere to one another and to vessel walls by interactions between integrin receptors on the cell surface and the Arg-Gly-Asp (RGD) sequence of extracellular matrix proteins (for

---

\*To whom correspondence should be addressed.

reviews, see Ruoslahti and Pierschbacher, 1986, 1987; Hynes, 1987; Hemler, 1990). The glycoprotein IIb/IIIa complex (Gp-IIb/IIIa) is the principal integrin receptor on the platelet surface. The extracellular matrix proteins which bind to platelet Gp-IIb/IIIa include fibrinogen, fibronectin, von Willebrand factor, and vitronectin. Fibrinogen appears to be the most important of these proteins with respect to platelet aggregation in circulation because of its abundance (Plow et al., 1986). Studies have shown that inhibition of fibrinogen binding to platelets with either antibodies (Coller, 1985; Gold et al., 1988; Yasuda et al., 1988; Coller et al., 1989) or RGD-based inhibitors (Bush et al., 1989; McGoff et al., 1989; Shebuski et al., 1989a,b) is an effective antithrombotic strategy. In addition to platelet aggregation, interactions between RGD-containing proteins and integrin receptors play an important role in development (Armant et al., 1986; Duband et al., 1986), tumor cell metastasis (Humphries et al., 1986), microbial invasion and disease (Ouaissi et al., 1986), platelet aggregation (Gardner and Hynes, 1985; Pytela et al., 1986), vascular proliferation and wound healing (Cheresh, 1985) and bone resorption (Sato et al., 1990).

Echistatin is a 49-amino acid protein (ECESGPCCRNCKFLKEGTICKRARGDDMDDYCNKGTCDPCRNPHKGPAT) isolated from the saw-scaled viper *Echis carinatus*. It is a member of a family of snake venom proteins that inhibit platelet aggregation (Huang et al., 1987; Gan et al., 1988; Shebuski et al., 1989a; Dennis et al., 1990). The tripeptide unit Arg-Gly-Asp is found in positions 24–26 and the protein contains eight cysteines. Since platelet aggregation is a key step in thrombus formation, it is of interest to understand the details of echistatin inhibition on the molecular level.

NMR spectroscopy is playing an increasingly important role in the determination and characterization of the 3D structure and dynamics of proteins (Wüthrich, 1986; Nirmala and Wagner, 1988; Kay et al., 1989; Clore et al., 1990b; Clore and Gronenborn, 1991a; Palmer et al., 1991; Barbato et al., 1992; Berglund et al., 1992; Kordel et al., 1992; Powers et al., 1992; Redfield et al., 1992; Schneider et al., 1992; Stone et al., 1992; Wagner et al., 1992). To generate structures of high accuracy and precision, it is important to have a large number of experimental constraints, including NOEs and torsion angle restraints (Clore and Gronenborn, 1991b). In echistatin, the number of NOEs is fewer than might be expected for a 49-residue protein and therefore only low-resolution structures can be generated (Chen et al., 1991; Cooke et al., 1991, 1992; Dalvit et al., 1991; Saudek et al., 1991a,b). The small number of NOEs is a reflection of the fact that large portions of the protein are quite mobile or flexible. In this paper, we present the 3D structure of echistatin and relate the motional averaging effects that are implicit in solution structures by calculating a theoretical order parameter for recognition-site residues from the ensemble of solution structures. The order parameter for the loop region that contains the recognition site derived from the solution structures is compared with order parameters derived from  $^{15}\text{N}$  relaxation experiments. The internal motion parameters for Ala<sup>23</sup>, Gly<sup>25</sup> and Asp<sup>26</sup> are obtained from  $^{15}\text{N}$  relaxation measurements and the overall correlation time of echistatin is derived from fluorescence measurements. Knowledge of both the structure *and* dynamics of echistatin is necessary in order to determine the role of flexibility in integrin-RGD interaction processes.

## MATERIALS AND METHODS

### *NOE constraints*

Echistatin was obtained by solid-phase synthesis (Garsky et al., 1989). The purity of the peptide was assessed by HPLC and was found to be greater than 95%. NOESY spectra (Anil Kumar et al., 1980) or pre-TOCSY NOESY spectra (Otting and Wüthrich, 1987) were recorded with echistatin dissolved in either 90% H<sub>2</sub>O/10% D<sub>2</sub>O or 99.996% D<sub>2</sub>O at a concentration of approximately 2 mM, pH = 3.1, at 27 °C. NMR experiments were run on a Varian VXR500 spectrometer at Rutgers University. Quadrature detection was applied to the  $t_2$  dimension and sign discrimination in  $t_1$  was achieved using the time-proportional phase incrementation (TPPI) method (Redfield and Kunz, 1975; Marion and Wüthrich, 1983). For each experiment, 2048 data points with 512  $t_1$  increments were recorded. FIDs were zero-filled to 2048 real data points in both dimensions, prior to Fourier transformation. Fourier transformation and integration of cross-peak intensities were obtained with the software FELIX (Hare Research, Inc.).

NOE cross peaks were assigned to specific proton pairs based on our resonance assignments (Chen et al., 1991). Other resonance assignments of echistatin were published independently and were found to agree with ours (Cooke et al., 1991; Dalvit et al., 1991; Saudek et al., 1991b). Distance constraints were obtained, based on NOE cross-peak intensities. The ranges of the distance constraints were estimated as follows. For the NOE constraints involving labile amide protons, cross peaks observed in a 50-ms mixing time pre-TOCSY NOESY experiment were classified as 'strong' or 'medium', associated with an upper distance limit of 2.7 or 3.5 Å, respectively. Cross peaks observed in a 200-ms pre-TOCSY NOESY spectrum but not in the 50-ms pre-TOCSY NOESY spectrum were classified as 'weak', associated with an upper limit of 5.0 Å. For NOE constraints between nonlabile protons, cross peaks observed in NOESY spectra of 80 ms or less were calibrated using the NOE cross peak of a methylene proton pair and the upper limit was set at +20% of the calculated distances. An additional 0.5-Å correction was made to the NOEs involving methyl groups. For overlapping NOE cross peaks or NOE cross peaks that were observed in a 200-ms mixing time NOESY spectrum but not in an 80-ms mixing time spectrum, the upper limit was set to 5.0 Å. The lower limit of the distance constraints was set in all cases to the sum of the van der Waals radii, 2.0 Å. At the present stage, 230 interresidue NOEs have been identified in NOESY spectra with mixing times of up to 200 ms, including 104 NOEs between sequential residues and 126 NOEs between protons of nonsequential residues. Of the 126 nonsequential NOEs, 94 are between resonances that are more than five residues apart.

### *Torsional constraints and stereospecific assignments*

Twelve backbone  $\Phi$  angles were constrained based on the measured coupling constants (Chen et al., 1991).  $^3J_{C^{\alpha}H-C^{\beta}H}$  coupling constants were measured using a P.E.COSY experiment (Mueller, 1987; Marion and Bax, 1988) with echistatin dissolved in 99.996% D<sub>2</sub>O at a concentration of 2 mM. The experiment was run at 27 °C and pH = 3.1, with a 45° mixing pulse. Sign discrimination in the  $t_1$  dimension was achieved by the hypercomplex method (Mueller and Ernst, 1979; States et al., 1982). 4096 data points were taken in the  $t_2$  dimension and 512 increments were recorded in the  $t_1$  dimension. The FIDs were zero-filled to 4096 real points in the  $t_2$  dimension before Fourier transformation, resulting in a digital resolution of 1.27 Hz/point. The measured  $^3J_{C^{\alpha}H-C^{\beta}H}$

TABLE 1  
MEASURED C<sup>α</sup>H-C<sup>β</sup>H COUPLING CONSTANTS OF C<sup>β</sup> METHYLENE PROTONS

Residue	C <sup>β</sup> H (± 1.27 Hz) (higher field)	C <sup>β</sup> H (± 1.27 Hz) (lower field)	Residue	C <sup>β</sup> H (± 1.27 Hz) (higher field)	C <sup>β</sup> H (± 1.27 Hz) (lower field)
Cys <sup>2</sup>	6.8	7.1	Tyr <sup>31</sup>	9.3	4.0
Glu <sup>3</sup>	8.9	5.1	Cys <sup>32</sup>	~12	4.6
Cys <sup>7</sup>	~12	3.0	Asn <sup>33</sup>	4.0	3.3
Arg <sup>9</sup>	7.0	7.2	Lys <sup>35</sup>	9.5	4.8
Asn <sup>10</sup>	8.8	5.8	Asp <sup>38</sup>	6.9	5.6
Phe <sup>13</sup>	13.7	3.2	Asp <sup>39</sup>	4.3	11.3
Asp <sup>26</sup>	7.6	5.6	Pro <sup>40</sup>	overlap	4.2
Asp <sup>27</sup>	5.6	6.3	Asn <sup>42</sup>	9.1	5.7
Met <sup>28</sup>	overlap	4.6	Pro <sup>43</sup>	4.3	8.6
Asp <sup>29</sup>	3.2	10.3	His <sup>44</sup>	8.8	7.8
Asp <sup>30</sup>	12.1	3.8	Pro <sup>47</sup>	5.1	9.2

coupling constants are listed in Table 1 and stereospecific assignments (Wagner et al., 1987) of β-methylene protons are listed in Table 2.

#### *Hydrogen-bonding constraints*

Hydrogen bonds were included as distance constraints. The secondary structure of echistatin has been identified from NOE data, deuterium–hydrogen exchange rates, as well as J-coupling constant measurements, as described in a previous paper (Chen et al., 1991). The distances between the corresponding amide nitrogen and carbonyl oxygen pairs were constrained within the limit of  $2.9 \pm 0.2$  Å. Eight slowly exchanging amide protons were observed in the antiparallel sheet and the β-hairpin region. However, only five hydrogen-bonding constraints are included in the distance constraints, because the other three are in regions where the regular secondary structure appears to be distorted, based on the absence of interchain NOEs and small coupling constants. The identified CO-NH hydrogen-bonding pairs are 5CO to 8NH, 9CO to 12NH, 12CO to 9NH, 30CO to 20NH and 18CO to 32NH.

#### *Computational methods*

Echistatin contains eight cysteines, i.e., residues 2, 7, 8, 11, 20, 32, 37 and 39, comprising four disulfide bonds. For two of the disulfide bonds, 2–11 and 20–39, strong evidence was found in the NOESY spectra (Chen et al., 1991). The NOEs between the C<sup>β</sup> proton of Cys<sup>37</sup> and the two C<sup>β</sup> protons of Cys<sup>8</sup> were identified. The NOEs between the NH of Cys<sup>7</sup> and the C<sup>β</sup>H of Cys<sup>32</sup> were also observed. However, it is difficult to assign disulfide pairings involving residues Cys<sup>7</sup> and Cys<sup>8</sup> from NOESY spectra, because they are next to each other in the primary sequence. Therefore, two sets of disulfide pairings were used in the calculation in the DSPACE program (Hare Research, Inc.): (1) 2–11, 20–39, 7–32, 8–37; and (2) 2–11, 20–39, 8–32, 7–37. The disulfide bonds were introduced as chemical bonds in both the IMPACT (Levy et al., 1989; Kitchen et al., 1990) and the DSPACE program.

The input for the DSPACE program consisted of NOE constraints, hydrogen-bonding con-

TABLE 2  
STEREOSPECIFIC RESONANCE ASSIGNMENTS OF SOME  $\beta$ -METHYLENE PROTONS

Residue	H <sup><math>\beta</math>R</sup> (ppm)	H <sup><math>\beta</math>S</sup> (ppm)	$\chi^1$ ( $\pm 30^\circ$ )
Asp <sup>29</sup>	2.56	2.48	300
Tyr <sup>31</sup>	2.56	2.64	300
Cys <sup>39</sup>	2.64	2.93	180
Pro <sup>6</sup>	1.92	2.63	
Pro <sup>40</sup>	1.82	2.22	
Pro <sup>43</sup>	2.22	1.86	
Pro <sup>47</sup>	1.97	2.27	

straints, bond lengths and bond angles inherent in the covalent structure of the primary sequence, and the disulfide bonds of echistatin. All distance constraints were incorporated as square-well biharmonic potential terms in both the penalty function of the DSPACE program and in the molecular mechanics potential function of the IMPACT program. The methylene protons which had not been stereospecifically assigned were specified, so that protons could float between pro-*R* and pro-*S* positions. Thirty-five structures for each set of disulfide pairings were embedded and refined in DSPACE with 194 NOE constraints, identified at the first stage, and five hydrogen-bonding constraints. Once one of the disulfide pairings was chosen, based on violations of the covalent structure and experimental constraints, new NOEs were found, based on the initial structures, and the final number of NOEs used for further structure generation and refinement was 230. New structures were embedded and refined in DSPACE with 230 NOE constraints and five hydrogen-bonding constraints.

Twenty new structures calculated in DSPACE with 230 NOE constraints and five hydrogen-bonding constraints were further refined in the program IMPACT, using the molecular mechanics potential energy function with an additional 21 torsional constraints. Distances involving methyl protons, methylene protons or symmetric protons on aromatic rings were evaluated as intensity-weighted averages (Levy et al., 1989). The refinement with the IMPACT program consisted of two stages: molecular dynamics (MD) simulation and energy minimization. During the dynamics calculation, the electrostatic, hydrogen-bonding and the 1–4 interaction terms were turned off. The system was heated to 500 K over 0.25 ps, equilibrated for 2 ps and then cooled down to 0.1 K for 0.5 ps. The cutoff distance for the van der Waals interaction evaluation was 6.0 Å. The force constant for NOE constraints was 30 kcal/mol Å<sup>2</sup>. In order to better satisfy the torsional constraints, particularly at higher temperatures, a large force constant was chosen for this term, i.e., 100 kcal/mol rad<sup>2</sup>. This is consistent with previously reported values of torsional force constants, typically varying between 40 and 200 kcal/mol rad<sup>2</sup> (Clare et al., 1986; Holak et al., 1989). Molecular dynamics simulation was then followed by conjugate gradient minimization to an rms gradient of 0.1 Å, with all the molecular mechanics potential terms including electrostatic, hydrogen-bonding and 1–4 interactions. The cutoff distance for van der Waals interactions was 7.5 Å. The dielectric function used for the electrostatic interactions was distance dependent,  $\epsilon = 2.5 R_{ij}$ . During this stage of refinement, a force constant of 20 kcal/mol Å<sup>2</sup> was used for the NOE constraints. The molecular mechanics potential terms and violations of the experimental distance constraints for the 10 best structures are given in Table 3.

### Fluorescence measurements

Tyrosine fluorescence anisotropy was measured with an SLM 8000 photon-counting fluorometer operated in the T-format. An excitation wavelength of 280 nm (bandpass = 4 nm) was employed and sample emission was passed through a Schott WG320 filter (allowing transmission above 320 nm) to eliminate Raman scatter. Glan Thompson prism polarizers were used to polarize exciting light and monitor polarized components of emission. A sample of echistatin at pH 3.2 was prepared in 5 mM sodium acetate–acetic acid buffer. Echistatin concentration was determined from an ultraviolet spectrum of this sample, employing an extinction coefficient of  $1480 \text{ M}^{-1} \text{ cm}^{-1}$  for tyrosine at 280 nm (Mach et al., 1992). Fluorescence from the sample was corrected for background signal from buffer alone. The sample temperature was controlled with a circulating Neslab RTE-100 water bath and measured with a Fluke 51 K/J thermometer. Viscosities of water at different temperatures were obtained from a National Bureau of Standards table (Weast, 1975).

The tyrosine fluorescence lifetime ( $\tau$ ) of echistatin was measured at pH 3.2 and ambient temperature with an ISS K2 multifrequency phase-modulation fluorometer, equipped with a digital filter for data acquisition through a Fast Fourier Transform routine. Modulation frequencies ranging from 20 to 200 MHz, and a cross-correlation frequency of 80 Hz were employed. Tyrosine fluorescence of echistatin was excited at 280 nm and a Schott glass WG320 filter was placed in the emission path. *p*-Terphenyl ( $\tau = 1.05 \text{ ns}$ ) was used as the lifetime reference. Phase shifts and demodulation ratios were analyzed by multiexponential least-squares analysis (Lakowicz et al., 1984).

The echistatin concentration for both anisotropy and lifetime measurements was 1.1 mg/ml. An optical pathlength of 4 mm was used for absorption and the absorption of the sample was 0.12. Thus, inner filter effect was not significant.

### $^{15}\text{N}$ relaxation measurements

Echistatin with  $^{15}\text{N}$ -labeled Ala<sup>23</sup>, Gly<sup>25</sup> and Asp<sup>26</sup> was obtained by solid-phase synthesis, using

TABLE 3  
MOLECULAR MECHANICS POTENTIAL ENERGIES (kcal/mol) OF THE TEN BEST STRUCTURES, REFINED WITH IMPACT

Structure	Bond	Angle	Dihedral	LJ 1–4	EL 1–4	LJ 6–12	EL	HB	$\Sigma d_{\text{viol}} (\text{Å})$	>0.1 Å	>0.5 Å
echs144m	16	182	178	161	255	–99	–352	–7.0	2.9	6	0
echs145m	10	166	173	122	255	–144	–327	–7.0	2.3	4	0
echs147m	11	185	173	121	262	–147	–365	–7.0	2.2	7	0
echs151m	21	292	234	147	249	–37	–301	–0.2	4.3	13	0
echs154m	18	216	211	125	247	–97	–316	–5.9	3.2	10	0
echs155m	20	312	224	149	256	–59	–333	13.3	4.4	14	0
echs157m	12	167	192	137	264	–86	–366	–7.3	2.5	6	0
echs160m	18	279	231	211	250	–86	–331	–3.7	2.0	4	0
echs161m	16	249	207	130	254	–105	–329	–0.2	3.8	9	0
echs166m	10	182	199	130	254	–105	–357	–4.7	3.5	13	0
Average	15	223	202	143	255	–97	–391	–3.0	3.1	9	0
SD	4	56	23	27	5	34	15	6.2	0.9	4	0

labeled amino acid residues (Garsky et al., 1989). The sample was prepared by dissolving echistatin in 90% H<sub>2</sub>O/10% D<sub>2</sub>O at a concentration of about 2 mM, pH = 3.0. NMR experiments were carried out on a Bruker AMX 600 spectrometer, equipped for multichannel operation at 27 °C at the Scripps Research Institute.

<sup>15</sup>N T<sub>1</sub> and T<sub>2</sub> times and NOEs of the three <sup>15</sup>N-labeled residues were measured using the 1D version of published pulse sequences (Stone et al., 1992). T<sub>1</sub> values were measured from eight time delays of 2.0, 33.1, 95.3, 157.6, 250.9, 406.5, 593.2 and 779.9 ms. T<sub>2</sub> values were also measured from eight time delays, i.e., 4.0, 52.0, 102.0, 154.0, 202.0, 252.0, 302.0 and 408.0 ms. For each time delay in both T<sub>1</sub> and T<sub>2</sub> experiments, 256 scans were acquired. The steady-state NOEs were measured as the ratios of peak heights in the spectrum recorded with proton saturation to those in the spectrum recorded without saturation. A proton saturation of 3.96 ms was obtained using GARP-1. The recycle delay for all T<sub>1</sub>, T<sub>2</sub> and NOE experiments was 4.0 s, which is longer than five times the proton T<sub>1</sub> relaxation time.

Fourier transformation of the spectra, baseline correction and peak height measurements were performed using the software FELIX 2.05 (Hare Research, Inc.). Both T<sub>1</sub> and T<sub>2</sub> values were obtained by fitting the experimental decay of peak height with time to a single exponential decay. T<sub>1</sub> was obtained by least-square fitting of the three-parameter equation:

$$I(T) = I_{\infty} - [I_{\infty} - I_0] \exp(-T/T_1)$$

T<sub>2</sub> was obtained by least-square fitting of the two-parameter equation:

$$I(T) = I_0 \exp(-T/T_2)$$

Uncertainties in peak height measurements for T<sub>1</sub> and T<sub>2</sub> were estimated by repeating the first and the last time points (2 and 779.9 ms for T<sub>1</sub>, 4 and 408 ms for T<sub>2</sub>). For the determination of NOEs, average values and standard deviations from four separate measurements were calculated (Palmer et al., 1991; Stone et al., 1992).

## RESULTS AND DISCUSSION

### *Analysis of structures*

Echistatin contains eight cysteine residues at positions 2, 7, 8, 11, 20, 32, 37 and 39. Disulfide bonds between Cys<sup>2</sup>-Cys<sup>11</sup> and Cys<sup>20</sup>-Cys<sup>39</sup> are suggested by the NMR data (Chen et al., 1991). The remaining disulfide pairings could be residues 7-32/8-37 (set I) or 8-32/7-37 (set II). Structures, embedded and refined with simulated annealing and minimization in DSPACE, with each possible set of disulfide pairings were analyzed in terms of the violations of experimental constraints, and violations derived from the covalent structure of the primary sequence of echistatin. Analysis of known crystal structures suggests that the torsional angles of the disulfide bonds have a strong preference for values of ± 90° (Kominos et al., 1990). We tried to use this as a criterion for the identification of the correct disulfide pairing. However, after embedding and refinement with the DSPACE program, the disulfide torsion angles were not close to ± 90° in either set of structures. Apparently, the NOE distance constraints alone are not sufficiently restrictive to establish the correct conformational preference of the disulfide bond. The analysis of the five lowest energy structures for each disulfide pairing is summarized in Table 4. The structures

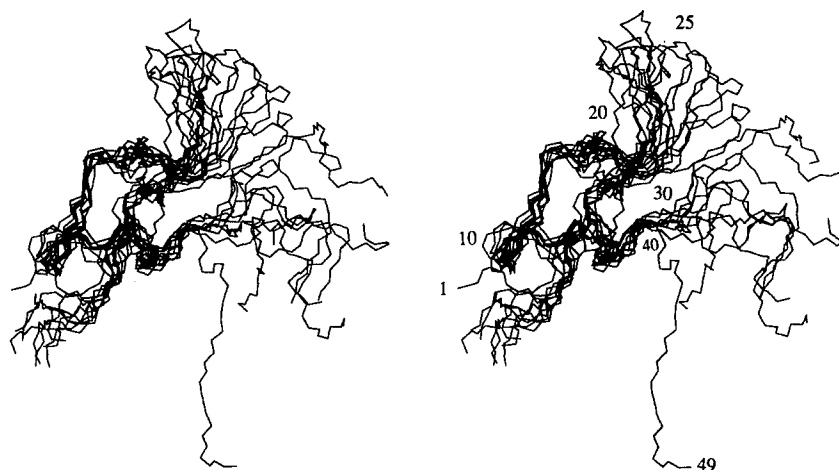


Fig. 1. Stereoview of a superposition of 10 structures of echistatin. The structures were superimposed to minimize the rmsd of backbone atoms of residues 8–20 and 30–40. The conformations of the N- and C-termini and the loop containing the RGD site are poorly defined relative to the core of the protein.

generated with set I disulfide pairings clearly show fewer violations of the covalent structure and experimental constraints than the structures generated with set II disulfide pairings. These results prompted us to choose the set I disulfide pairings as being correct. Similar results were found by Cooke et al. (1991), who determined the disulfide pairing in echistatin by a statistical analysis of the simulated annealing structures using XPLOR. More recent work by Calvete et al. (1992) suggested the same disulfide pairing by chemical means. A new, more sensitive chemical method was used by Gray (1993) to unambiguously confirm the pairing.

Once set I disulfide pairings were chosen, new NOEs were found based on these initial structures. The family of echistatin structures shown in Fig. 1 satisfies 230 interresidue distance constraints, five hydrogen-bonding constraints, and 21 torsional constraints. Figure 1 shows the superposition for the polypeptide backbone of the 10 lowest energy echistatin structures, refined with the IMPACT program following embedding and refinement in the DSPACE program. The

TABLE 4  
STATISTICS FOR THE BEST FIVE STRUCTURES FROM DSPACE OF THE TWO SETS OF DISULFIDE PAIRING

Disulfide pairing	Average total distance violation <sup>a</sup> (Å)	Standard deviation of total distance violation (Å)	Average no. of distance violation <sup>b</sup>		
			>1.0 Å	>0.5 Å	>0.1 Å
Set 1	21.5	4.9	0	0	0.8
Set 2	38.5	3.4	0	0.2	4.2

<sup>a</sup> The average is the sum of violation of the covalent structure, derived from the primary sequence and the violation of total experimental distance constraints. All violations have been converted to distance.

<sup>b</sup> The violation only refers to experimental distance violation.





Fig. 2. The overall fold of echistatin.  $\beta$ -strands are shown as ribbons, and the two short  $\beta$ -sheets are colored in red and blue, respectively. Heavy atoms of cysteine residues and disulfide bonds shown in yellow indicate the positions of the disulfide pairing. The model was generated on an SGI IRIS 4D workstation with the program MOLSCRIPT (Kraulis, 1991).

10 structures do not have violations of the NOE constraints greater than 0.5 Å. The backbone fold of the protein is well defined only for regions containing approximately residues 8–20 and 30–40. After the best fit superposition of the backbone atoms for residues 8–20 and 30–40, the average rms deviation of backbone atoms (C, C $^{\alpha}$ , N) for these residues is  $1.7 \pm 0.3$  Å and the average rms deviation of all atoms for the same region is  $2.8 \pm 0.4$  Å.

The backbone fold of echistatin and disulfide pairings are shown in Fig. 2. From the N-terminus, the structurally defined regions begin with a Type I  $\beta$ -turn in residues 5–8 (Chen et al., 1991). Following the turn is a  $\beta$ -hairpin in residues 8–14, with hydrogen bonding between residues 9 and 12. In addition, we have identified a tight turn in residues 9–12 as a Type I'  $\beta$ -turn (Chen et al., 1991). Residues 16 and 17 form a turn in our structures; the turn might be a half turn, based on the strong C $^{\alpha}$ H-to-NH NOE between residues 16 and 17, the NH-NH NOE between residues 17 and 18 and the C $^{\alpha}$ H-to-NH NOE between residues 16 and 18 (Wüthrich, 1986). Since no coupling constants are available for residues 16 and 17, this turn cannot be uniquely identified

and structural calculations do not give any conclusive answer. Residues 18–20 and 30–32 form a short antiparallel  $\beta$ -sheet (Chen et al., 1991). The short sheet is apparently distorted. Residues 21–29 form a loop, containing the RGD binding site. Following the sheet, residues 33–36 form a turn, as numerous short-range  $i$  to  $i + 2$  and  $i$  to  $i + 3$  NOEs are observed in this region. Residues 37–42, which comprise a second binding site (Pro<sup>40</sup>-Pro<sup>43</sup>) (Gould et al., 1990), form another loop. From residue 42 on, the structure is not very well defined.

The global fold of echistatin and its 3D structure have been reported earlier by us (Chen et al., 1991), by Saudek et al. (1991a,b) and by Cooke et al. (1991,1992). The overall conformation of our structures is similar to that of the reported structures. The disulfide pairings that are selected in our structures and in those of Cooke et al. (1992) are the same, whereas Saudek et al. (1991a) were unable to distinguish between set I and set II disulfide pairings. Small differences in secondary structure exist between our structures and reported structures (Chen et al., 1991; Dalvit et al., 1991; Cooke et al., 1991,1992; Saudek et al., 1991a). All the reported structures agree in that the RGD binding site is in a loop connecting residues 21–29. Conformational studies have been reported on a number of other peptides and proteins that are active in the inhibition of platelet aggregation (Reed et al., 1988; Genest et al., 1989; Negre et al., 1989; Mickos et al., 1990; Aumailley et al., 1991; Bogusky et al., 1992,1993; McDowell and Gadek, 1992; Mizutani et al., 1992; Peishoff et al., 1992; Siahaan et al., 1992). In these short RGD-containing peptides, the RGD sites tend to form turn-like structures. In addition, the RGD binding site in the protein kistrin is located at the apex of a turn (Adler et al., 1991). The turn-like structure of the RGD site might be important for the cell-binding activity.

As seen in Fig. 1, certain regions of the protein are relatively well defined, whereas other regions, such as the loop region and the terminal ends, are not. This is further observed in Table 5. The average rms deviation among backbone atoms of all residues is approximately 4 Å between structures before and after the MD refinements. However, the average rms deviation among backbone atoms of the structured regions (residues 8–20 and 30–40) is only 1.6 Å between

TABLE 5  
COMPARISON OF THE RMSD OF BACKBONE ATOMS BETWEEN STRUCTURES BEFORE AND AFTER DYNAMICS REFINEMENT USING IMPACT

Structure	Backbone rmsd (Å)	
	Residues 8–20, 30–40	All residues
echs144	1.56	3.66
echs145	1.74	5.97
echs147	1.95	4.39
echs151	1.68	3.00
echs154	1.48	5.68
echs155	1.76	4.37
echs157	1.18	4.50
echs160	1.17	1.55
echs161	1.74	4.56
echs166	1.68	3.47
Mean	1.59	4.12

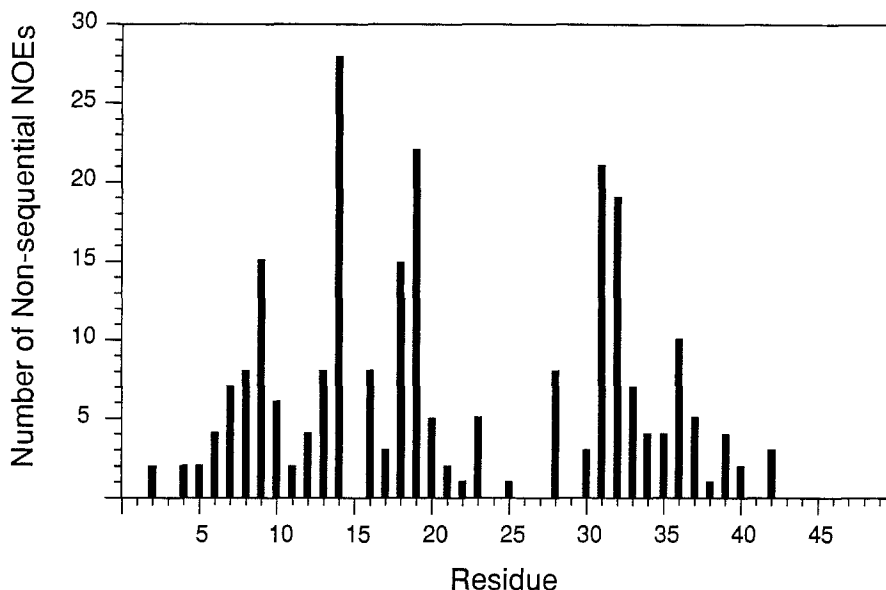


Fig. 3. Plot of total number of nonsequential, interresidue NOEs identified for each residue from NOESY spectra obtained at 200 ms or less. Structured regions of the protein are characterized by large numbers of NOEs. The nine-residue loop containing the RGD moiety is found at residues 21–29 and exhibits few nonsequential NOEs.

structures before and after the dynamics refinement. The much smaller changes in the structured regions during the MD refinement are probably due to the presence of conformational constraints in the structured regions. The N- and C-terminal regions and the loop connecting the two strands of the antiparallel  $\beta$ -sheet are poorly defined, as would be expected from the fact that these regions lack nonsequential NOE constraints (Chen et al., 1991). Therefore, these regions change considerably during the MD calculation. After MD refinement with IMPACT, the disulfide torsion angles lie within the appropriate range  $|90^\circ \pm 10^\circ$ . The large variation of the N- and C-terminal regions and the nine-residue loop containing the RGD sequence suggests that the computational methods that were used to generate and refine the structures performed a reasonably good sampling of the conformational space.

#### *Dynamics of the active site*

Determining the mobility of the active site is a key issue in order to better characterize those features of the Arg-Gly-Asp unit that are compatible with receptor binding. Numerous interresidue NOEs are observed for the structured regions of the protein, while very few interresidue NOEs are observed for the termini and the loop containing the Arg-Gly-Asp sequence (Fig. 3). These data, as well as coupling constants of approximately 6 Hz in the RGD region, are consistent with the view that the loop containing the active site is conformationally mobile (Chen et al., 1991).

A manifestation of the lack of NOE constraints in the loop region (Fig. 3) is that the backbone fold, in the ensemble of solution structures shown in Fig. 1, is not well defined for this region of the protein. While the standard approach to measuring motional parameters in macromolecules is via NMR relaxation experiments, motional averaging effects are implicit in the

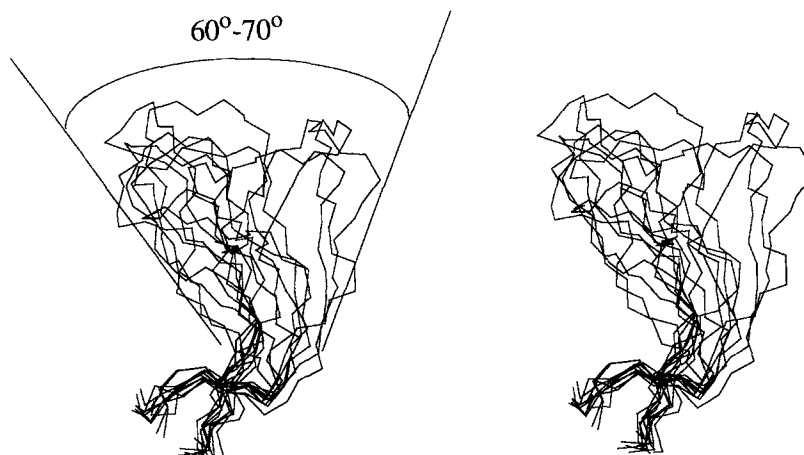


Fig. 4. Superposition of the  $\beta$ -sheet and the loop containing the RGD site of 20 structures. The structures were superimposed to minimize the rmsd of backbone atoms of residues 18–20 and 30–32. The flexibility of the loop is mainly lateral and within a range of approximately 60–70°.

ensemble of structures, generated during the determination of a protein structure from NMR data. The lack of well-defined structure is often ascribed to the presence of mobility. We can attempt to quantify these motional effects in solution structures by calculating a theoretical order parameter from a set of solution structures which satisfy the NOE and torsional constraints. When considering an ensemble of protein structures which satisfy NMR-derived constraints (the ‘solution structure’ of the protein), it is almost a matter of definition that regions of the protein which are very well determined are said to be more rigid, whereas the lack of resolution of other regions is often ascribed to the presence of mobility. To date there has been no attempt to make this qualitative description more precise. It is possible to calculate generalized order parameters from the coordinates of the ensemble of structures which satisfy the NMR-derived constraints. Under the assumption that the protein is able to interconvert between the various structures in the ensemble on the same time scale as that probed in the NMR relaxation experiment, the generalized order parameters calculated from the ‘solution structure’ may be compared with those calculated from  $T_1$ ,  $T_2$  relaxation experiments. We have carried out such an analysis for echistatin.

To calculate a theoretical order parameter, a motional model for the loop region is chosen, based on the structures. The loop containing the active site RGD is anchored on a well-structured  $\beta$ -sheet and has a flexible orientation, as shown in Fig. 4. The orientational flexibility in the ensemble of ‘solution structures’ indicates that the local motions of the loop are mainly lateral and are within a range of approximately 60–70°. A generalized order parameter for the NH vectors of the RGD site was calculated, assuming a ‘wagging’ motion of the loop within an arc of 60–70° as shown in Fig. 4, using the following function (Levy et al., 1981):

$$S^2 = \frac{4\pi}{5} \sum_{n=-2}^2 |\langle Y_2^n(\theta_{\text{mol}}(0)\phi_{\text{mol}}(0)) \rangle|^2$$

where the  $Y_2^n$  are second-order spherical harmonics,  $\theta$  and  $\phi$  are polar angles of the internuclear

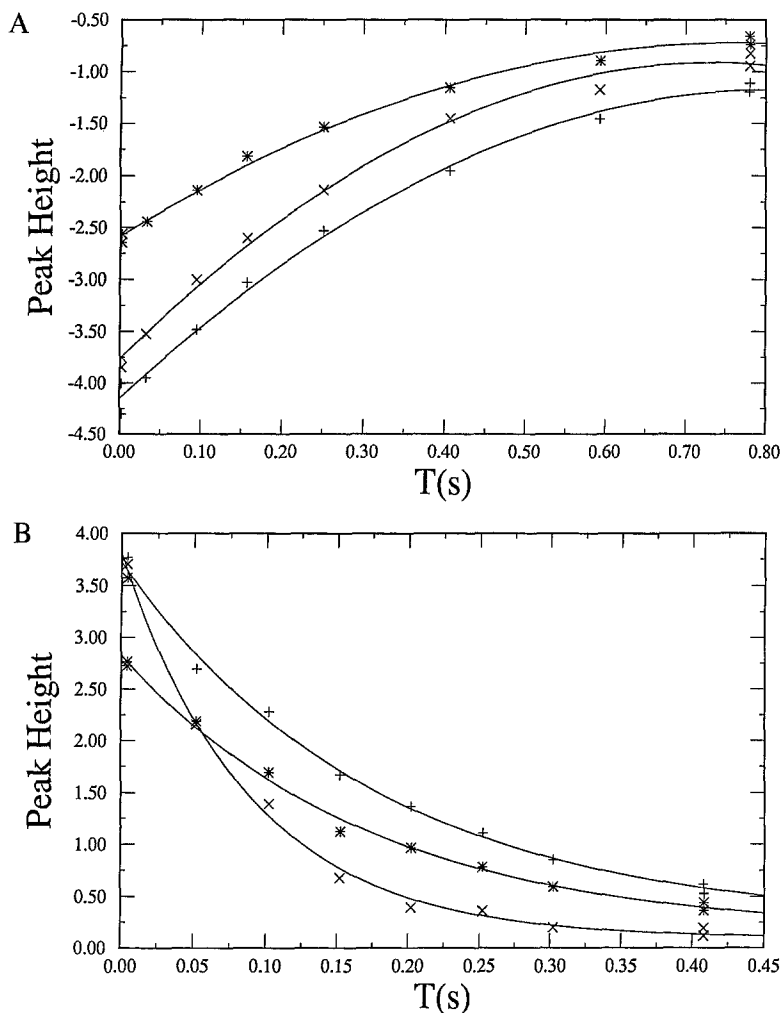


Fig. 5. Plots of peak intensity versus relaxation time for (A)  $T_1$  and (B)  $T_2$  measurements. The three residues are represented by (+) for glycine, (x) for alanine and (\*) for aspartic acid.

vector with respect to a fixed molecule axis, and the angular brackets represent a correlation function. All orientations of the loop are assumed to be equally likely, so that  $\theta$  is allowed to vary between 0 and 60°. The calculated order parameter from this 'wagging' model, based on the solution structures, is about 0.7.

To correlate flexible regions of the 'solution structure' with experimental relaxation data, order parameters for the loop region, calculated from the ensemble of structures shown in Fig. 1, were compared with order parameters from  $^{15}\text{N}$  relaxation data obtained for Ala<sup>23</sup>, Gly<sup>25</sup> and Asp<sup>26</sup>. The  $^{15}\text{N}$   $T_1$  and  $T_2$  relaxation data are shown in Fig. 5 and the  $T_1$ ,  $T_2$  and NOE values are listed in Table 6. The MD information contained in  $T_1$  and  $T_2$  relaxation measurements is obtained using the model-free analysis of Lipari and Szabo (1982a,b). In the model-free formalism, the spectral density function for a molecule undergoing isotropic tumbling is given by:

$$J(\omega) = \frac{S^2 \tau_c}{1 + \omega^2 \tau_c^2} + \frac{(1 - S^2) \tau}{1 + \omega^2 \tau^2}$$

where  $S^2$  is the generalized order parameter for the motional averaging of the  $^1\text{H}$ - $^{15}\text{N}$  internuclear vector,  $\tau_c$  is the tumbling time and  $\tau = \tau_c \tau_e / (\tau_c + \tau_e)$ , where  $\tau_e$  is the effective correlation time describing the internal motions.

In the analysis of the relaxation data, the overall correlation time of the protein,  $\tau_c$ , is usually estimated by averaging the values of the  $T_1/T_2$  ratios that are obtained for the individual residues (Kay et al., 1989). In our case,  $\tau_c$  was not obtained from the  $T_1/T_2$  ratios, as the small number of residues studied would not provide an accurate estimate of the overall correlation time. Instead, an external measure of the overall correlation time was obtained from fluorescence measurements. We note that the tumbling time  $\tau_c$ , probed in NMR relaxation and fluorescence anisotropy measurements, is determined by the second-order spherical harmonics correlation functions, so that  $\tau_c$  determined by the two methods will be equivalent for an isotropically rotating body.

Fluorescence measurements in echistatin were performed on the single tyrosine residue. Upon excitation at 280 nm, a typical tyrosine fluorescence spectrum with a maximum at 305 nm was obtained. Steady-state tyrosine fluorescence anisotropy of echistatin was measured at nine different temperatures between 4 and 49 °C. Circular dichroism measurements indicated that there was no change in secondary structure over this temperature range (data not shown). Fluorescence anisotropy varied from 0.184 at 4.4 °C to 0.144 at 48.8 °C (standard deviation = 0.001 anisotropy units for 10 or more measurements at each temperature). A Perrin plot of  $1/\text{anisotropy}$  versus temperature/viscosity was linear (correlation coefficient = 0.996) and the apparent limiting anisotropy, extrapolated from this plot, is 0.212.

The average tyrosine fluorescence lifetime ( $\tau_{av}$ ) of echistatin was determined to be 1.14 ns (SD = 0.05 ns), based on measurements at 12 modulation frequencies ranging from 30 to 200 MHz. The apparent correlation time for the overall rotational rate of echistatin was calculated for 25 °C from the Perrin equation (Lakowicz, 1983) to be  $4.1 \pm 0.5$  ns, using a limiting anisotropy of 0.212 and a  $\tau_{av}$  of 1.14 ns, and allowing for an error of  $\pm 0.002$  and  $\pm 0.1$  ns in anisotropy and lifetime measurements, respectively. An overall correlation time of 4.1 ns for echistatin appears to be somewhat large, considering that larger proteins have correlation times that are smaller or equal in size to that of echistatin. For example, the correlation times for ubiquitin and eglin c, which contain 76 and 70 residues respectively, are both 4.1 ns (Peng and Wagner, 1992; Schneider et al., 1992). However, based on the data for thioredoxin and glucose permease IIA domain, there appears to be no exact relationship between protein size and overall correlation time. Although thioredoxin and glucose permease IIA domain are quite different in size (108 and 164 residues, respectively), both have similar correlation times of 6.4 and 6.24 ns, respectively (Stone et al., 1992, 1993).

The spectral density function for the analysis of the relaxation data was determined from the magnitude of the NOEs, and from a comparison of the experimental  $T_1/T_2$  ratio of individual residues to the ratio calculated from the  $\tau_c$ , obtained from fluorescence measurements. The experimental  $T_1/T_2$  ratios of the three labeled residues are not equal to the calculated ratio of 2.75, based on fluorescence measurements (Table 6). This result indicates that  $\tau_e$  is not negligible and/or a chemical exchange term contributes significantly to  $T_2$ . In addition, the NOE term is very sensitive to the effective correlation time  $\tau_e$ . When  $\tau_e$  is negligible ( $< 20$  ps), the maximum

TABLE 6  
RELAXATION DATA AND DYNAMICS PARAMETERS

	$T_1^{-1}$ (s <sup>-1</sup> )	$T_2^{-1}$ (s <sup>-1</sup> )	NOE	$S^2$	$\tau_e$ (ns)	$R_{ex}$ (s <sup>-1</sup> )
Ala <sup>23</sup>	2.56 ± 0.08	11.11 ± 4.08	0.54 ± 0.01	0.29 ± 0.01	2.66 ± 0.14	6.58 ± 0.37
Gly <sup>25</sup>	2.44 ± 1.27	9.06 ± 1.58	0.35 ± 0.02	0.50 ± 0.02	1.19 ± 0.05	4.44 ± 0.15
Asp <sup>26</sup>	2.86 ± 1.01	5.88 ± 1.40	0.46 ± 0.02	0.46 ± 0.02	1.67 ± 0.08	1.17 ± 0.13

possible <sup>1</sup>H-<sup>15</sup>N NOE is calculated to be 0.77 for an overall correlation time of 4.1 ns at 600 MHz. The observed NOEs are much smaller than this value, again indicating that  $\tau_e$  is significant.

Internal motional parameters (Table 6) which include the generalized order parameter  $S^2$ , the effective correlation time  $\tau_e$ , and the chemical exchange term  $R_{ex}$ , that best fit the  $T_1$ ,  $T_2$  and NOE values were obtained by minimization of the target function (Palmer et al., 1991; Stone et al., 1992):

$$\chi^2 = \sum_{i=1}^n \left[ \frac{(R_{1obs} - R_{1cal})^2}{\sigma_1^2} + \frac{(R_{2obs} - R_{2cal})^2}{\sigma_2^2} + \frac{(NOE_{obs} - NOE_{cal})^2}{\sigma_{NOE}^2} \right]$$

where  $R_{obs}$  represents the measured relaxation values and  $R_{cal}$  the calculated values for  $T_1$ ,  $T_2$  and NOE, the  $\sigma_i$ 's are the standard deviations obtained from repeated independent measurements, and the sum runs over the three labeled resonances in echistatin. The overall correlation time was 4.1 ns, based on the fluorescence measurement. The uncertainties were estimated by using the method of Palmer et al. (1991). The  $\chi^2$  values for the three residues are very small (0.00, 0.02 and 0.20), indicating good agreement between the calculated and experimental relaxation parameters.

We have obtained an experimental measure of the mobility of the residues in the active site by <sup>15</sup>N relaxation measurements (Table 6). In previous dynamics studies of proteins (Kay et al., 1989; Clore et al., 1990a,b; Kordel et al., 1992; Stone et al., 1992), residues that exhibit a slow motion component with  $\tau_e > 50$  ps, <sup>1</sup>H-<sup>15</sup>N NOE values significantly less than the theoretical maximum value,  $T_1/T_2$  ratios not close to the mean  $T_1/T_2$  ratio of the whole molecule, and small  $S^2$  values (0.05 to 0.75) are usually found in structurally highly mobile regions of a protein. The relaxation measurements for echistatin with  $S^2$  values of 0.3–0.5 indicate that the three residues are highly mobile. This is consistent with the observed absence of long-range NOE constraints and averaged coupling constants. Comparison of the order parameter deduced from the family of solution structures and the experimental order parameter indicates that the motion detected in the relaxation experiments is more extensive than the idealized (one-dimensional) model of the RGD loop 'wagging' motion suggested by the picture of the superposed solution structures (Fig. 4). Thus, in addition to the overall reorientation of the loop other motions are contributing to the relaxation detected in the <sup>15</sup>N relaxation experiments. Two approaches to developing a more detailed picture of the motions contributing to the relaxation, based on analyzing the echistatin solution structures, are being pursued. First, parameters for more extensive (multidimensional) models for the motion of the <sup>15</sup>N-<sup>1</sup>H internuclear vectors can be extracted by fitting the observed reorientation of the corresponding vectors in the common molecular frame, defined by the superposed solution structures, to analytical models. Second, the generalized order parameter can

be calculated directly from the solution structures, after reorienting the structures into the common molecular frame, without recourse to an analytical model. In preliminary studies we have found, however, that 10 solution structures are insufficient to obtain convergence of calculated order parameters.

## CONCLUSIONS

This is the first study that we are aware of that has attempted to extract motional information from a set of NMR solution structures, generated from NOE constraints, which can then be compared with motional information extracted from relaxation measurements. We note a related effort (Hyberts et al., 1992) to quantify flexibility by analyzing the variation in torsional coordinates of a set of solution structures. In attempting to quantify motional information contained in a set of protein solution structures, it is necessary to keep in mind motional time scales. For order parameters extracted from relaxation experiments, or those calculated directly from MD simulations, there are clearly defined time scales; up to nanoseconds for the former and the duration of the simulation for the latter. In contrast, for order parameters calculated from solution structures superposed in a common molecular frame, there is not a well-defined time scale. For example, slower motions which are not detectable in a  $^{15}\text{N}$  relaxation experiment may well contribute to the dispersion in the solution structures. The lack of NOE constraints due to sources unrelated to motion will contribute to the apparent flexibility, which further complicates the comparison of order parameters extracted from a set of solution structures with those extracted from relaxation experiments or MD simulations. By analyzing and comparing generalized order parameters extracted from all three kinds of data, i.e., NMR relaxation experiments, MD simulations, and NMR solution structures, we hope to develop a consistent picture of the extent of motional flexibility of the RGD active site on multiple time scales. The flexibility of the binding site may be a crucial factor in Gp IIb/IIIa inhibition by echistatin and by other Arg-Gly-Asp-containing peptides.

## ACKNOWLEDGEMENTS

This work has been supported by a grant from Merck Research Laboratories and the Searle Scholar Fund/Chicago Community Trust to J.B. and by NIH GM-30580 to R.L. J.B. thanks the Camille and Henry Dreyfus Foundation for a Teacher-Scholar Award and the Alfred P. Sloan Foundation for a Research Fellowship. We would like to thank Dr. Peter Wright for kindly allowing us to use the spectrometers at the Scripps Research Institute, and Dr. Arthur Palmer for the use of his program to fit a model-free theory to heteronuclear NMR relaxation data.

## REFERENCES

- Adler, M., Lazarus, R.A., Dennis, M.S. and Wagner, G. (1991) *Science*, **253**, 445–448.  
Anil Kumar, Ernst, R.R. and Wüthrich, K. (1980) *Biochem. Biophys. Res. Commun.*, **95**, 1–6.  
Armant, D.R., Kaplan, H.A., Mover, H. and Lennarz, W.J. (1986) *Proc. Natl. Acad. Sci. USA*, **83**, 6751–6755.  
Aumailley, M., Gurrath, M., Müller, G., Calvete, J., Timpl, R. and Kessler, H. (1991) *FEBS Lett.*, **291**, 50–54.  
Barbato, G., Ikura, M., Kay, L.E., Pastor, R.W. and Bax, A. (1992) *Biochemistry*, **31**, 5269–5278.  
Berglund, H., Kovacs, H., Dahlman-Wright, K., Gustafsson, J. and Hard, T. (1992) *Biochemistry*, **31**, 12001–12011.



- Bogusky, M.J., Naylor, A.M., Pitzengerger, S.M., Nutt, R.F., Brady, S.F., Colton, C.D., Sisko, J.T., Anderson, P.S. and Veber, D.F. (1992) *Int. J. Pept. Protein Res.*, **39**, 63–76.
- Bogusky, M.J., Naylor, A.M., Mertzman, M.E., Pitzengerger, S.M., Nutt, R.F., Brady, S.F., Colton, C.D. and Veber, D.F. (1993) *Biopolymers*, **33**, 1287–1297.
- Bush, L.R., Holahan, M.A., Kanovsky, S.M., Mellott, M.J., Garsky, V.M. and Gould, R.J. (1989) *Circulation*, **80**, 11–23.
- Calvete, J.J., Wang, Y., Mann, K., Schafer, W., Niewiarowski, S. and Stewart, G.J. (1992) *FEBS Lett.*, **309**, 316–320.
- Chen, Y., Pitzengerger, S.M., Garsky, V.M., Lumma, P.K., Sanyal, G. and Baum, J. (1991) *Biochemistry*, **30**, 11625–11636.
- Cheresh, D.A. (1985) *Proc. Natl. Acad. Sci. USA*, **84**, 6471–6475.
- Clore, G.M., Nilges, M., Sukumaran, D.K., Brünger, A.T., Karplus, M. and Gronenborn, A.M. (1986) *EMBO J.*, **5**, 2729–2735.
- Clore, G.M., Szabo, A., Bax, A., Kay, L.E., Driscoll, P.C. and Gronenborn, A.M. (1990a) *J. Am. Chem. Soc.*, **112**, 4989–4991.
- Clore, G.M., Driscoll, P.C., Wingfield, P.T. and Gronenborn, A.M. (1990b) *Biochemistry*, **29**, 7387–7401.
- Clore, G.M. and Gronenborn, A.M. (1991a) *Prog. NMR Spectrosc.*, **23**, 43–92.
- Clore, G.M. and Gronenborn, A.M. (1991b) *Science*, **252**, 1390–1399.
- Coller, B.S. (1985) *J. Clin. Invest.*, **76**, 101–108.
- Coller, B.S., Folts, J.D., Smith, S.R., Scudder, L.E. and Jordan, R. (1989) *Circulation*, **80**, 1766–1774.
- Cooke, R.M., Carter, B.G., Martin, D.M.A., Murray-Rust, P. and Weir, M.P. (1991) *Eur. J. Biochem.*, **202**, 323–328.
- Cooke, R.M., Carter, B.G., Murray-Rust, P., Harsborn, M.J., Herzyk, P. and Hubbard, R.E. (1992) *Protein Eng.*, **5**, 473–477.
- Dalvit, C., Widmer, H., Bovermann, G., Breckenridge, R. and Metternich, R. (1991) *Eur. J. Biochem.*, **202**, 315–321.
- Dennis, M.S., Henzel, W.J., Pitti, R.M., Lipari, M.T., Napier, M.A., Deisher, T.A., Bunting, S. and Lazarus, R.A. (1990) *Proc. Natl. Acad. Sci. USA*, **87**, 2471–2475.
- Duband, J.-L., Rocher, S., Chen, W.-T. and Yamada, K.M. (1986) *Science*, **233**, 467–470.
- Gan, Z.-R., Gould, R.J., Jacobs, J.W., Friedman, P.A. and Polokoff, M.A. (1988) *J. Biol. Chem.*, **263**, 19872–19882.
- Gardner, J.M. and Hynes, R.O. (1985) *Cell*, **42**, 439–448.
- Garsky, V.M., Lumma, P.K., Freidinger, R.M., Pitzengerger, S.M., Randall, W.C., Veber, D.F., Gould, R.J. and Friedman, P.A. (1989) *Proc. Natl. Acad. Sci. USA*, **86**, 4022–4026.
- Genest, M., Marion, D., Caille, A. and Ptak, M. (1989) *Colloq. INSERM, Forum Pept.*, **174**, 415–418.
- Gold, H.K., Coller, B.S., Yasuda, T., Saito, T., Fallon, J.T., Guerrero, R.C., Zinskinbd, A.A. and Collen, D. (1988) *Circulation*, **77**, 670–677.
- Gould, R.J., Polokoff, M.A., Friedman, P.A., Huang, T.-E., Holt, J.C., Cook, J.T. and Niewiarowski, S. (1990) *Proc. Soc. Exp. Biol. Med.*, **195**, 168–171.
- Gray, W.R. (1993) *Protein Sci.*, **2**, 1749–1755.
- Hemler, M.E. (1990) *Annu. Rev. Immunol.*, **8**, 365–400.
- Holak, T.A., Gondol, D., Otlewski, J. and Wilusz, T. (1989) *J. Mol. Biol.*, **210**, 635–648.
- Huang, T.-F., Holt, J.C. and Lukasiewicz, S. (1987) *J. Biol. Chem.*, **262**, 16157–16163.
- Humphries, M.J., Olden, K. and Yamada, K.M. (1986) *Science*, **233**, 467–470.
- Hyberts, S.G., Goldberg, M.S., Havel, T.F. and Wagner, G. (1992) *Protein Sci.*, **1**, 736–751.
- Hynes, O.R. (1987) *Cell*, **48**, 549–554.
- Kay, L.E., Torchia, D.A. and Bax, A. (1989) *Biochemistry*, **28**, 8972–8979.
- Kitchen, D.B., Hirata, F., Westbrook, J.D., Levy, R.M., Kofke, D. and Yarmush, M. (1990) *J. Comput. Chem.*, **11**, 1169–1180.
- Kominos, D., Bassolino, D.A., Levy, R.M. and Pardi, A. (1990) *Biopolymers*, **29**, 1807–1822.
- Kordel, J., Skelton, N.J., Akke, M., Palmer, A.G. and Chazin, W.J. (1992) *Biochemistry*, **31**, 4856–4866.
- Kraulis, P.J. (1991) *J. Appl. Crystallogr.*, **24**, 945–949.
- Lakowicz, J.R. (1983) *Principles of Fluorescence Spectroscopy*, Plenum Press, New York, NY.
- Lakowicz, J.R., Laczko, G., Cherek, H., Gratton, E. and Limkeman, M. (1984) *Biophys. J.*, **46**, 463–477.
- Levy, R.M., Karplus, M. and Wolynes, P.G. (1981) *J. Am. Chem. Soc.*, **103**, 5998–6012.
- Levy, R.M., Bassolino, D.A. and Kitchen, D.B. (1989) *Biochemistry*, **28**, 9361–9372.
- Lipari, G. and Szabo, A. (1982a) *J. Am. Chem. Soc.*, **104**, 4546–4559.

- Lipari, G. and Szabo, A. (1982b) *J. Am. Chem. Soc.*, **104**, 4559–4570.
- Mach, H., Middaugh, C.R. and Lewis, R.V. (1992) *Anal. Biochem.*, **200**, 74–80.
- Marion, D. and Wüthrich, K. (1983) *Biochem. Biophys. Res. Commun.*, **113**, 967–974.
- Marion, D. and Bax, A. (1988) *J. Magn. Reson.*, **80**, 528–533.
- McDowell, R.S. and Gadek, T.R. (1992) *J. Am. Chem. Soc.*, **114**, 9245–9253.
- McGoff, M.A., Allen, B.T., Sicard, G.A., Anderson, C.B. and Santoro, S.A. (1989) *Circulation*, **80**, 11–23.
- Mickos, H., Bahr, J. and Luning, B. (1990) *Acta Chem. Scand.*, **44**, 161–164.
- Mizutani, R., Shimada, I., Ueno, Y., Yoda, M., Kumagai, H. and Arata, Y. (1992) *Biochem. Biophys. Res. Commun.*, **182**, 966–973.
- Mueller, L. and Ernst, R.R. (1979) *Mol. Phys.*, **38**, 963–992.
- Mueller, L. (1987) *J. Magn. Reson.*, **72**, 191–196.
- Negre, E., Marion, D., Roche, A.C., Monsigny, M. and Mayer, R. (1989) *Colloq. INSERM, Forum Pept.*, **174**, 575–578.
- Nirmala, N.K. and Wagner, G. (1988) *J. Am. Chem. Soc.*, **110**, 7557–7558.
- Otting, G. and Wüthrich, K. (1987) *J. Magn. Reson.*, **75**, 546–549.
- Ouaisi, M.A., Cornette, J., Afchain, D., Capron, A., Gras-Massa, H. and Tartar, A. (1986) *Science*, **234**, 603–607.
- Palmer III, A.G., Rance, M. and Wright, P.E. (1991) *J. Am. Chem. Soc.*, **113**, 4371–4380.
- Peishoff, C.E., Ali, F.E., Bean, J.W., Calvo, R., D'Ambrosio, C.A., Eggleston, D.S., Hwang, S.M., Kline, T.P., Koster, P.F., Nichols, A., Powers, D., Romoff, T., Samanen, J.M., Stadel, J., Vasko, J.A. and Kopple, K.D. (1992) *J. Med. Chem.*, **35**, 3962–3969.
- Peng, J. and Wagner, G. (1992) *Biochemistry*, **31**, 8671–8686.
- Plow, E.F., Ginsberg, M.H. and Marguerie, G.A. (1986) In *Biochemistry of Platelets* (Eds, Philips, D.R. and Shuman, M.A.) Academic Press, New York, NY, pp. 225–256.
- Powers, R., Clore, G.M., Stahl, S.J., Wingfield, P.T. and Gronenborn, A. (1992) *Biochemistry*, **31**, 9150–9157.
- Pytela, R.M., Pierschbacher, M.D., Ginsberg, M.H., Plow, E.F. and Ruoslahti, E. (1986) *Science*, **231**, 1559–1562.
- Redfield, A.G. and Kunz, S.D. (1975) *J. Magn. Reson.*, **19**, 250–254.
- Redfield, C., Boyd, J., Smith, L.J., Smith, R.A.G. and Dobson, C.M. (1992) *Biochemistry*, **31**, 10431–10437.
- Reed, J., Hull, W.E., Von der Lieth, C.-W., Kubler, D., Suhai, S. and Kinzel, V. (1988) *Eur. J. Biochem.*, **178**, 141–154.
- Ruoslahti, E. and Pierschbacher, M.D. (1986) *Cell*, **44**, 517–518.
- Ruoslahti, E. and Pierschbacher, M.D. (1987) *Science*, **238**, 491–497.
- Sato, M., Sardana, M.K., Grasser, W.A., Garsky, V.M., Murray, J.M. and Gould, R.J. (1990) *J. Cell Biol.*, **111**, 1713–1723.
- Saudek, V., Atkinson, R.A. and Pelton, J.T. (1991a) *Biochemistry*, **30**, 7369–7372.
- Saudek, V., Atkinson, R.A., Lepace, P. and Pelton, J.T. (1991b) *Eur. J. Biochem.*, **202**, 329–338.
- Schneider, D.M., Dellwo, M.J. and Wand, A.J. (1992) *Biochemistry*, **31**, 3645–3652.
- Shebuski, R.J., Ramjit, D.R., Bencen, G.H. and Polokoff, M.A. (1989a) *J. Biol. Chem.*, **264**, 21550–21556.
- Shebuski, R.J., Berry, D.E., Bennett, D.B., Romoff, T., Storer, B.L., Ali, F. and Samanen, J. (1989b) *Thromb. Haemostasis*, **61**, 183–188.
- Siahaan, T.J., Chakrabarti, S. and Van der Velde, D. (1992) *Biochem. Biophys. Res. Commun.*, **187**, 1042–1047.
- States, D.J., Haberkorn, R.A. and Ruben, D.J. (1982) *J. Magn. Reson.*, **48**, 286–292.
- Stone, M.J., Fairbrother, W.J., Palmer III, A.G., Reizer, J., Saier, M.H. and Wright, P.E. (1992) *Biochemistry*, **31**, 4394–4406.
- Stone, M.J., Chandrasekhar, K., Holmgren, A., Wright, P. and Dyson, J.H. (1993) *Biochemistry*, **32**, 426–435.
- Wagner, G., Braun, W., Havel, T.F., Schaumann, T., Gö, N. and Wüthrich, K. (1987) *J. Mol. Biol.*, **196**, 611–639.
- Wagner, G., Hyberts, S.G. and Havel, T.F. (1992) *Annu. Rev. Biophys. Biomol. Struct.*, **21**, 167–198.
- Weast, R.C. (Ed.) (1975) *Handbook of Chemistry and Physics*, 56th ed., CRC Press, Boca Raton, FL, p. F-49.
- Wüthrich, K. (1986) *NMR of Proteins and Nucleic Acids*, Wiley, New York, NY.
- Yasuda, T., Gold, H.K., Fallon, J.T., Leinbach, R.H., Guerrero, J.L., Scudder, L.E., Kanke, M., Sheahly, D., Ross, M.J., Collen, D. and Collier, B.S. (1988) *J. Clin. Invest.*, **81**, 1284–1291.